Communications in Computational Chemistry
Commun. Comput. Chem., Vol. 1, No. 2, 88–96
doi: 10.4208/cicc.2025.88.01
Regular Article

Quantum Dynamics of Water from Møller-Plesset Perturbation Theory via a Neural Network Potential

Mengxu Li[1,2], Jinggang Lan[1,4,*], David M. Wilkins[3,*], Vladimir V. Rybkin[4,5,*], Marcella Iannuzzi[4] and J ü rg Hutter[4]

[1]*Faculty of Synthetic Biology, Shenzhen University of Advanced Technology, Shen-zhen, Guangdong, China;*

[2]*School of Physics, Dalian University of Technology, Dalian 116024, China;*

[3]*Atomistic Simulation Centre, School of Mathematics and Physics, Queen's University Belfast, Belfast BT7 1NN, Northern Ireland, United Kingdom;*

[4]*Department of Chemistry, University of Zurich, Winterthurerstrasse 190, Zurich 8057, Switzerland;*

[5]*Current address: HQS Quantum Simulations GmbH, Rintheimer Str. 23, D-76131 Karlsruhe, Germany.*

[*] Corresponding authors: vladimir.rybkin@quantumsimulations.de (V. Rybkin), d.wilkins@qub.ac.uk (D. Wilkins), jinggang.lan@suat-sz.edu.cn (J. Lan)

Received on 29 March 2025; Accepted on 24 April 2025

Abstract: We report the static and dynamical properties of liquid water at the level of second-order Møller-Plesset perturbation theory (MP2) with classical and quantum nuclear dynamics using a neural network potential. We examined the temperature-dependent radial distribution functions, diffusion, and vibrational dynamics. MP2 theory predicts over-structured liquid water as well as a lower diffusion coefficient at ambient conditions compared to experiments, which may be attributed to the incomplete basis set. A better agreement with experimental structural properties and the diffusion constant are observed at an elevated temperature of 340 K from our simulations. Although the high-level electronic structure calculations are expensive, training a neural network potential requires only a few thousand frames. This approach shows great potential, requiring modest human effort, and is straightforwardly extensible to other simple liquids.

PACS: 82.20.-w, 82.60.Lf, 61.20.Gy, 47.11.-

Key words: MP2, machine learning, quantum simulation, diffusion coefficient.

1. Introduction

Water, a prerequisite for our existence on this planet, plays a vital role in nearly all environmental, biochemical, physical processes, whether in bulk or at interfaces [1,2]. Water's anomalous properties, such as high surface tension, elevated viscosity, and maximum density at a specific temperature, render this ubiquitous liquid a molecular mystery, driving sustained studies across scientific disciplines [2,3]. Despite the ability to characterize these macroscopic properties through the persistent advancements in scientific instruments and theoretical methods, resolving the atomistic picture—particularly the structure of water—remains a significant challenges and continues to spark considerable debate.

The most fundamental question in gaining a microscopic comprehension of water is what are the structure and dynamics of the hydrogen bonding network. Experimental studies have primarily relied on characterization techniques including Raman spectroscopies [4,5], X-ray diffraction [6,7], and nuclear magnetic resonance [8], but remain constrained by limitations in temporal and spatial resolution [5]. Hence, a close synergy between theoretical methods and experimental results is imperative for a concerted effort toward a unified picture of water.

Computational science persists in developing a sufficiently accurate aqueous model, primarily carrying out molecular dynamics (MD) simulations with ab initio calculations or empirical force-field. [3, 9–20] It is thus not unexpected that numerous theoretical models of water have been reported in the literature, such as the TIP*n*P family [21–23], SPC [24, 25], q-AQUA [12–14] and MB-Pol [26]. Nevertheless, the density functional theory (DFT) holds its status as a cornerstone reference due to its exactness for ground-state properties in principle. A key point is that DFT in practice requires approximations to be made in the exchange-correlation energy, which critically governed the precision of calculations. The accuracy progressively improves along the Jacob's ladder of electronic structure theory, ascending from the local density approximation (LDA) through generalized gradient approximations (GGAs), meta-GGAs, and hybrid functionals, extending beyond to double hybrids, random phase approximation (RPA), and correlated wave function methods, such as second-order Møller-Plesset perturbation theory (MP2).

The selection for exchange-correlation functional exhibits considerable sensitivity in describing aqueous structural properties, from gas phase to solid. LDA is deemed unacceptable due to its overbinding of the water dimer, leading to an overstructured liquid water and a very small diffusion constant [27, 28]. GGA performs better than LDA, but still shows systematic errors in characterizing intermolecular water interactions. MD simulations at the GGA level, without dispersion corrections, require a substantial increase in temperature above 300 K to keep water in the liquid state. For example, PBE, a widely adopted functional, can reproduce experimental radial distribution functions (RDFs) and density at T = 440 K and P = 0.3 GPa, [29]. Even with the addition of Grimme's dispersion correction (DFT-D3) to PBE, which fails to markedly improve the structure of water [30], elevated temperatures are still required to reproduce these properties [30, 31]. BLYP-D3, with its reasonable performance in describing water properties [27], also requires simulations at 360 K to reproduce the correct RDF [32]. As a modification of the PBE functional, revPBE-D3 tends to perform best for RDF, density, and diffusion coefficient at ambient conditions without increasing the temperature [27, 30]. However, the results are highly sensitive to the particular choice of dispersion functional, as evidenced by the revPBE+DRSLL functional tending to overestimate the volume of ice VIII by 20%. [27] Recent developments in computational power and methodology have made it possible to climb higher rungs of the ladder beyond GGA, namely meta-GGA, hybrid functionals, and many-body correlated methods [33]. Perdew and co-workers proposed the non-empirical SCAN meta-GGA functional achieves remarkable accuracy for weak interaction systems [34]. SCAN functional yields the correct ordering of densities between liquid water and ice, at the same time predicting quantitative agreement with experiments at an elevated temperature of 330 K [35]. Despite its relatively higher accuracy, the bare SCAN functional still systematically overbinds water clusters [36]. Moreover, adding rVV10 to SCAN further exacerbates the overbinding, leading to a noticeable over- estimation of the density of liquid water [37]. Building on methods refinements, density-corrected SCAN calculation, presented by Paesani and co-workers, has improved accuracy to a level comparable to the "gold standard" coupled-cluster theory, which correctly describes water from the gas to the liquid phase through minimizing density-driven errors [36]. Simultaneously, some empirically parametrized meta-GGA functionals such as B97M with rVV10 correction also appear to perform quite well [38].

At hybrid functional level, the revPBE0-D3 functional is able to predict the correct experimental RDF and density at room temperature [39]. However, revPBE0-D3 still un- derestimates the temperature-dependent density of water by about 5% [40], which may be attributed to the choice of van der Waals interactions.The hybrid functional combined with rVV10 van der Waals interactions better reproduced the experimental equilibrium density of water through fine-tuning the empirical parameter [41]. Beyond hybrid functionals, including virtual orbitals allows for long-range van der Waals dispersion interactions from parameter-free ab-initio calculations. With tremendous computational cost, one can reach the fifth rung of the ladder with methods such as RPA and MP2. The MP2 theory, incorporating stronger dispersion interactions, provides excellent predictions of the density at room temperature and calculates radial distribution functions that are in reasonable agreement with experimental data [42]. Previous studies suggest that "MP2 water" is denser and cooler at ambient conditions compared both with experiment and with "DFT water" [43]. In addition to the underlying electronic structure theory, another issue is the accurate account of the quantum nature of the nuclei [44,45]. Due to the light mass of hydrogen nuclei, neglecting the pronounced nuclear quantum effects (NQEs) in aqueous systems [45]. The competition between intermolecular and intramolecular quantum effects, along with the challenge of accurately assessing these NQEs, could be one of the largest sources of errors [46,47]. For instance, the inclusion of NQEs induces subtle differences in RDFs, especially those that involve hydrogen atoms [44]. In a classical simulation, to produce a change in the RDF equivalent to that obtained by considering NQEs, the temperature has to be increased approximately 30 K [10,35]. Proton fluctuations along the covalent bond direction in quantum simulations also increase almost 10-fold. In addition, Voth et al. verified that higher temperatures do not accurately replicate NQEs at room temperature, which is evident in different three-body correlations as well as dynamics. [48] Regarding the reactivity of water, "classical" water is more basic than "quantum" water (i.e., water in nature) with a pH of 8.6, which is about a 30-fold change in the ionization constant [44]. Similar phenomena have also been

detected at metal-water interfaces [49] and for electron transfer in aqueous solutions [50]. Therefore, the inclusion of NQEs is often necessary to achieve high accuracy in molecular dynamics simulations.

Path integral molecular dynamics (PIMD) is a method to incorporate quantum mechanics into molecular dynamics by mapping each quantum particle onto a classical representation [51]. Combining electronic structure theory with PI methods is exceedingly computationally expensive, as each particle is represented by several classical replicas and each replica requires a separate on-the-fly electronic structure calculation. For this reason, high-level electronic structure calculations coupled with quantum nuclear dynamics have been made possible in the last decade [39]. Thanks to the recent development of neural network potentials (NNPs) [52,53], an extensive study using a high-quality functional beyond local DFT is feasible even when combined with path-integral molec- ular dynamics. The densities of water as predicted by NNP trained on revPBE0-D3 data agree with the experiment to within 3% for both liquid water and ice Ih and Ic [40]. Accurate and efficient quantum vibrational spectra of water can also be obtained for bulk and interfacial systems through NNPs trained on ab initio data [54, 55]. Quantum dynamics simulations through Behler-Parrinello Neural Network force field from a fifth-rung electronic structure level have provided an accurate determination of the structure, diffusion, and vibrational features of water and aqueous solvated electron [56,57].

In this work, the structural and dynamical properties of bulk water have been studied by means of classical MD and thermostatted ring polymer molecular dynamics (TRPMD) simulations via an NNP in terms of radial distribution functions, diffusion coefficient, and vibrational dynamics at different temperatures. At ambient conditions, MP2 theory predicts overstructured liquid water, which might be due to an incomplete basis set. Only quantum simulations conducted at 340 K produce structural properties and diffusion coefficients that are in better agreement with experimental results at room temperature. Our theoretical results provide a dialectical conclusion on the MP2 level, opening up new possibilities for the further refinement and enhancement of the theoretical framework.

2. Computational details

All MD simulations are performed using the i-PI code [58, 59] interfaced with LAMMPS [60], which implements the NNP potential using N2P2 [61]. The details of the simula- tion, including the static and dynamic properties as well as the training of the NNP, are provided below.

To achieve efficient canonical sampling while minimally perturbing the dynamics, the temperature of classical MD simulations was controlled using a stochastic velocity rescaling (SVR) thermostat [62], with a time constant of 1000 fs. A timestep of 0.5 fs was used. In the frame of PIMD method, thermostatted ring polymer molecular dynamics (TRPMD) was developed to capture dynamical properties incorporating NQEs [63]. The use of 64 ring-polymer beads was sufficient to converge the properties of interest, even at low temperatures [40,64]. The Parrinello-Rahman mass matrix was adjusted to shift all normal mode frequencies to to ωNM = 14000 cm^{-1}. The temperature was controlled using the global path integral Langevin equation (PILE-G) thermostat attached to all the non-centroid normal modes [65], with a time constant of 1000 fs. TRPMD has been shown to predict accurate vibrational dynamics of liquid water [39,66].

The density of liquid water has been calculated from classical nuclei MD via an NNP based on MP2 theory. MD simulations were performed using a cubic cell containing 128 water molecules with the NPT ensemble at 1 atm for 12 different temperatures between 240 and 350 K. For each temperature, the trajectory is about 1 ns long.

Dynamical properties are calculated based on a 300 ps trajectory at each temperature for additional vibrational density of states (VDOS) calculations. The dynamical properties of liquid water can be measured by the diffusion coefficient (D) which can be estimated by Einstein's relation:

$$D = \frac{1}{6t}|\boldsymbol{r}(t) - \boldsymbol{r}(0)|^2 . \qquad (2.1)$$

Where r(t) are the atomic positions at time t, and r(0) is the atomic positions at 0. Due to the finite-size effect on diffusion, the extrapolated self-diffusion coefficient D(∞) can be expressed as the finte system diffusion D(L) plus a correction:

$$D(\infty) = D(L) + \frac{\xi k_b T}{6\pi\beta\eta L} \qquad (2.2)$$

where L is the length of the simulation cell, kb is Boltzmann constant, T is temperature, ξ= 2.83729 for cubic box and η is the experimental shear viscosity as taken from Ref. [67].

The VDOS from classical MD or TRPMD is calculated using the Fourier transform of the velocity autocorrelation

$$C_{vv}(\omega) = \int \langle \boldsymbol{v}(\tau)\cdot\boldsymbol{v}(t+\tau)\rangle_\tau e^{-i\omega t}dt, \qquad (2.3)$$

with the quantum autocorrelation function computed using the centroid velocity v.

The quality of training sets plays a pivotal role in constructing reliable machine learning potentials for MD simulations. The starting point for our NNP is that of Ref. 57, at the MP2 level, which contains 14085 datasets from classical nuclei molecular dynamics [68], 100 datasets from path-integral molecular dynamics simulations [57] under NVT ensemble at 300K. The reference data obtained at room temperature may be highly correlated, leading to incorrect dynamics at temperatures other than 300 K. The potential was re- trained by generating a large set of configurations of 64 molecules at temperatures from 240 K to 350 K using replica exchange molecular dynamics [69] in the NPT ensemble. An additional 1000 structures were selected using CUR decomposition based on their atomic fingerprints [70]. MP2 calculations [71,72] with triple-zeta quality correlation-consistent basis sets [73] were carried out using CP2K [74,75]. The performance of the NNP shown in the Supporting Information, was evaluated based on root mean square error for both energies and forces, yielding 1.35 meV/H2O in energies and 92.84 meV/Å.

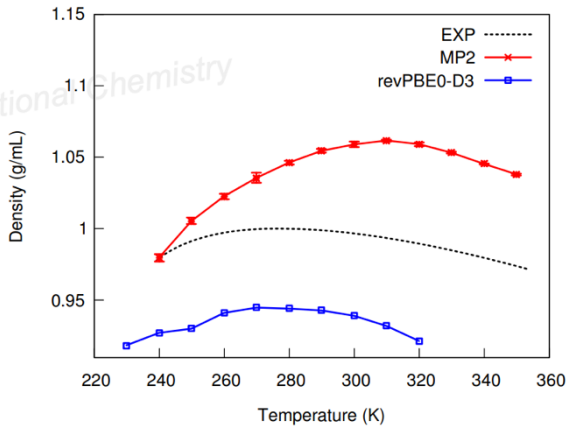

Figure 1. The density of liquid water predicted by MP2 simulations in NPT ensemble with comparison to the experimental data [77], and the result from the revPBE0-D3 [40].

3. Results

3.1 Structure of MP2 water at different temperatures

Accurately describing the density of water at the DFT level has been challenging, and only a few potential energy surfaces, such as q-AQUA-pol [13] and MB-pol [76] have demonstrated consistency with experimental results at finite temperatures. The density of liquid water predicted by classical simulations at the MP2 level is shown in Fig. 1, with water at room temperature having a density of 1.058 g/cm3. Both MP2 and revPBE0-D3 calculations with classical nuclei exhibit deviations of approximately 5% from the experimental density at room temperature. Specifically, MP2 calculation tends to overestimate the density, while revPBE0-D3 tends to underestimate it. In order to better compare with the experiment, we used 128 water molecules at experimental density (0.997 g/mL) to perform following simulations.

In general, MP2 is more likely to overbind noncovalent complexes. To shed light on the structure of water at different temperatures, the radial distribution functions (RDFs) of oxygen-oxygen, oxygen-hydrogen, and hydrogen-hydrogen pairs have been calculated, as shown in Fig.2. The imperfect agreement between MP2 simulations and the experimental structure may be attributed to an insufficient basis set. Calculations are carried out using a triple-ζ basis set. MP2 is known to overestimate dispersion when a relatively small basis set is applied. [80–83] Previous studies indicate that as the basis set increases from double-ζ to triple-ζ to quadruple-ζ, the mean absolute error in the binding energies relative to the complete basis set (CBS) values decreases from 2.18 to 1.74 to 0.99 kcal/mol for the water clusters (n=2–10). The relatively small basis set overestimates the binding energies compared to the CBS [83]. The global minima of water clusters (n=2–6) at the MP2 level agree with the CCSD(T) level of theory [84]. However, MP2 systematically contracts the nearest-neighbor O–O separation in water clusters by 0.005–0.022 Å with the average of 0.016 Å. In this respect, MP2 tends to overestimate binding energies compared to CCSD(T) results at the same quality of basis set (aug-cc-pVDZ) [84]. When the binding energies are extrapolated to the CBS limit, both

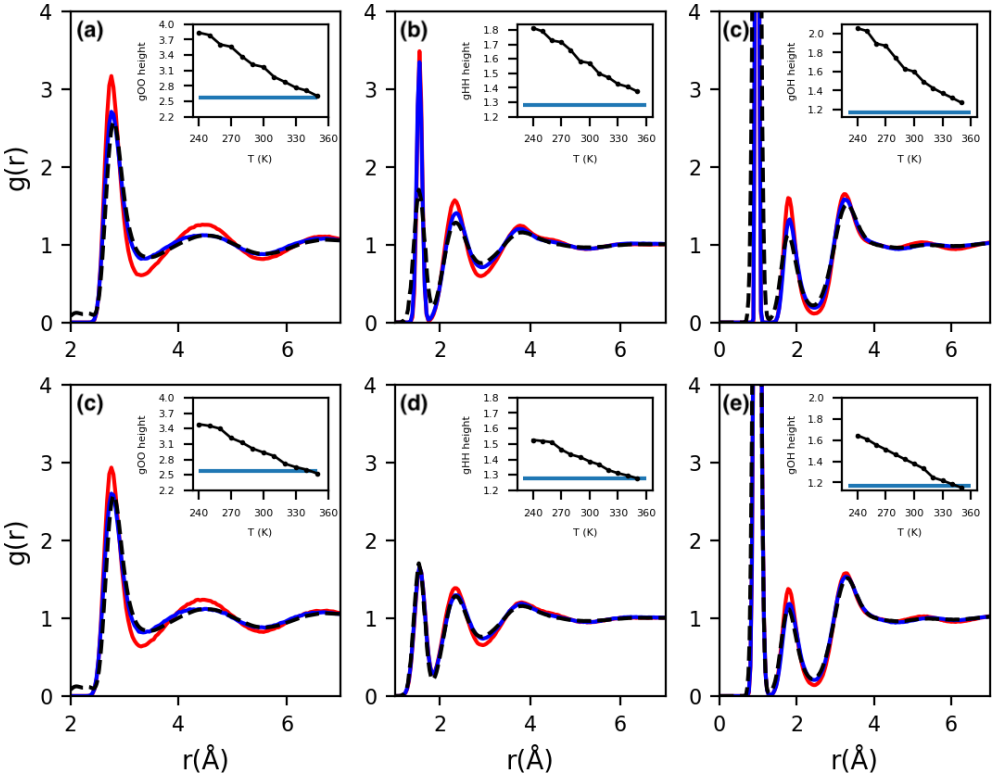

Figure 2. Radial distribution function gOO(r) (a,c), gHH(r) (b,d) and gOH(r) (c,e) as obtained from classical (a–c) and quantum (c–e) simulations at 300 K (red) and 340 K (blue) from 128 water models, in comparison to the experimental values at room temperature (black dashed line). [78, 79] Subplots show the heights at different temperatures of gOO(r) at the first peak, gHH(r) and gOH(r) at second peak. The light blue lines in subplots represent RDF heights of the experimental value at room temperature.

MP2 and CCSD(T) predict very similar values. The differences between the two methods are generally lower than 0.5 kcal/mol [84].

Given the fact MP2 with triple-ζ overbinds and overestimates the dispersion, it is not surprising that MP2 water at room temperature over-structures and behaves like ice. The temperature dependence of the RDFs from 240 to 350 K was also examined in Fig. 2. The RDFs are strongly affected by the temperature with a negative correlation at each peak. Temperature effects are more pronounced at the first peaks of gOO(r) which concerns the structure of the first solvation shell. As the temperature increases, the water becomes less ordered with a relatively lower intensity of gOO(r) at the first peak. NQEs broaden and weaken the intensity of the first peaks in gOO(r) and these effects are more pronounced at a lower temperature. A temperature difference of 30 K in classical simulations is required to give the same height of gOO(r) as in quantum simulations, indicating that the quantum simulation is "hotter" [10,35]. Classical MD simulations of water are often carried out at an elevated temperature to mimic the quantum effect of oxygen and yield an improved description of the local structure of water [10].

Indeed, NQEs are particularly pronounced in systems involving light atoms. The classical simulation, conducted at an elevated temperature of 330 K, may fail dramatically to replace the quantum simulation at 300 K, especially for describing the gHH(r) and

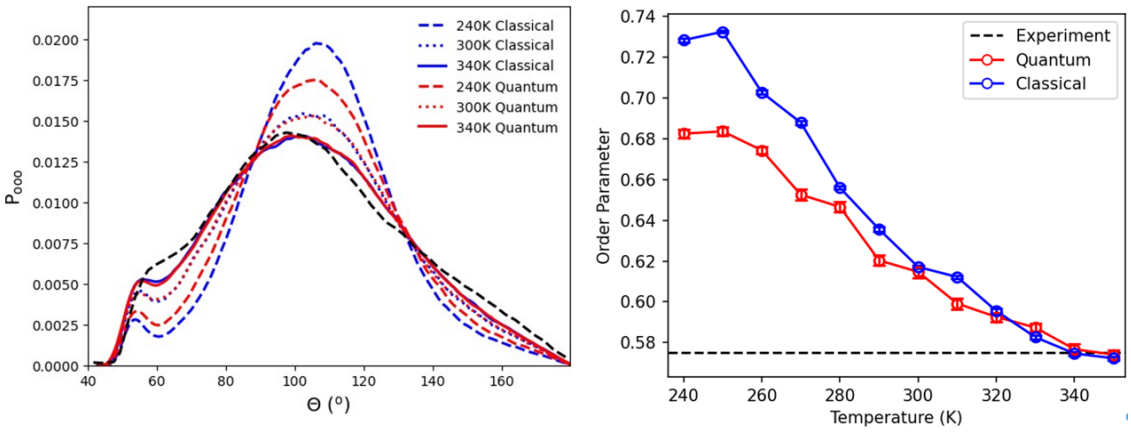

Figure 3. The oxygen–oxygen–oxygen triplet angular distribution as obtained from classical and quantum dynamics at multiple temperatures. The resulting tetrahedral order parameter of liquid water is shown as a function of temperature. The experimental data at 298 K are marked in black dashed line as comparison [79].

gOH(r) [10]. As shown in Fig.2(b,d), NQEs significantly broaden the first and second peaks of gHH(r) and gOH(r). Similarly, we also plot the temperature dependence of the height of the second peaks of gHH(r) and gOH(r). It is evident that the temperature difference may be more than 70 K for gHH(r) (See subplots in Fig.2(b,d)) and 50 K for gOH (See subplots in Fig.2(c,e)) at the second peak of the RDFs. More importantly, the broadening of the first peaks of gHH(r) and gOH(r) cannot be reproduced with an elevated temperature even up to 70 K. Classical MD simulations only sample within the range of the thermal energy kT, which is far below the zero-point energy of an O–H stretch. Accurate RDFs can be achieved from MP2 theory with a higher temperature of 340 K, as shown by our classical and quantum dynamics. The experimental RDFs at room temperature are given in the dashed black lines in Fig. 2. The calculated gOO(r), gHH(r) and gOH(r) at 340 K match with the experimental value at room temperature.

To further understand the local structure of the water molecules, we calculate the distribution oxygen-oxygen-oxygen triplet angles

$$q=1-\frac{3}{8}\sum_{i=1}^{3}\sum_{j=i+1}^{4}(cos(\theta_{ij}+\frac{1}{3})^2, \qquad (3.1)$$

within the first solvation shell and the tetrahedral order parameter q, defined as where θ_{ij} is the angle formed by the central water molecules and its two neighboring water molecules i and j. To calculate the distribution of oxygen-oxygen-oxygen triplet angles within the first solvation shell, we take the cutoff distance of two oxygen atoms of 3.35 Å, which yields an average coordination number of 4. An order parameter of q = 1 defines a perfect tetrahedral local environment, and q decreases as the structure of water becomes less ordered and tetrahedral.

As shown in Fig.3, the experimental triplet angles show a weak shoulder at around 60° and a broad strong peak at around 100°. We present the calculated Pooo at three different temperatures – 240 K, 300 K, and 340 K. At the lower temperature of 240 K, NQEs strongly adjust the local environment of water, resulting in a less ordered water structure. The order parameter as estimated from quantum simulations is about 0.68 which is lower than that of 0.72 from classical simulations. The difference of local parameters becomes less with increasing the temperature. At room temperature, MP2 predicts a local parameter of 6.15 for quantum simulations (6.17 for classical), which is higher than the prediction from the fragment-based MP2/aug-cc-pVDZ simulation [85,86]. The inconsistency may come from the choice of basis sets and the employment of fragmentation methods. Beyond room temperature, the local parameter from classical and quantum simulations is almost identical (see Fig.3). The local order parameter at 340 K (quantum=0.577, qclassical=0.575) predict almost exact number compared to the experimental value of 0.570. The calculated triplet angles distributions predict an accurate line shape at around 100°, but a weaker shoulder at 56° instead of 60°.

3.2 Dynamical properties

It is difficult to converge the diffusion coefficient using ab initio molecular dynamics due to its high computational cost, especially when combined with high-level electronic structure theory beyond standard GGA. Diffusion coefficients from high-level electronic structure theory have been only made available by using a multiple time stepping (MTS) method. For instance, Marsalek and Markland carried out revPBE0-D3 calculations using ring-polymer contraction with MTS methods [39]. The calculated diffusion coefficient of liquid water at 300 K is determined to be 2.67 and 2.29×10^{-5} cm^2/s from classical and quantum simulations respectively. The inclusion of NQEs decreases the diffusion co- efficient by 30% [39]. Del Ben and co-workers combined a hybrid functional (PBEW1- D3) with MP2, using fast (0.25 fs) and slow (2.5 fs) time steps to calculate the dynamical property of MP2 water [68]. Their analysis is based on two trajectories of each roughly 10 ps as obtained in the NVE ensemble, and the self-diffusion constant values obtained are 0.67 and 0.77×10^{-5} cm^2/s at 300 and 307 K, respectively. At room temperature, our simulations predict a diffusion constant of 0.629 (0.693) and 0.996 (1.060) $\times10^{-5}$ cm^2/s from classical and quantum dynamics (the quantities in brackets are after finite-size correction [87]), which is in fair agreement with previous simulations [68].

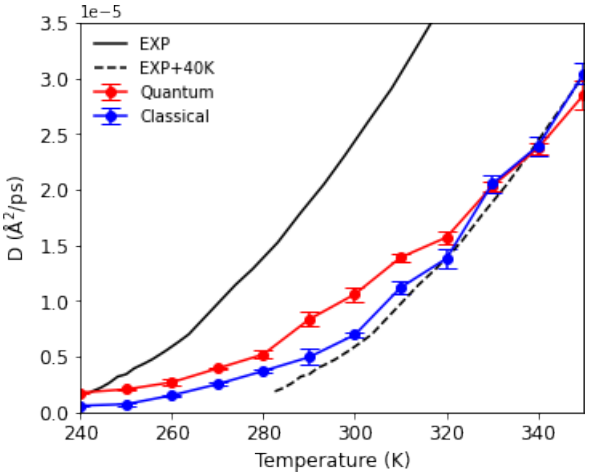

Figure 4. Temperature dependence of the diffusion coefficient after finte size correction as obtained from classical and quantum simulations, in comparison to the experimental values (black line) [88] and its shifted value by 40 K.

In fact, a classical MD simulation with a limited timescale of 10-20 ps may yield statistical error bars of more than 20% on dynamical quantities such as the diffusion coefficient. That may explain the minor inconsistency between our values and previous results [39,68]. Nevertheless, these values are below the experimental diffusion at room temperature, and more similar to a lower-temperature diffusion. We plot the temperature- dependent diffusion coefficient as obtained from classical and quantum dynamics in Fig.4. The diffusion constants are systematically underestimated by MP2 theory for both classical and quantum simulations. Previous studies show that NQEs contribute a 30% decrease to the self-diffusion of liquid water using revPBE0-D3 functional [39]. Unlike the revPBE0-D3 functional, the diffusion of water upon including NQEs at the MP2 theory is enhanced by 10–70% from 240 to 320 K, while a slow down of diffusion by 3–7% has been observed beyond 330 K.

Surprisingly, when the experimental diffusion constant is shifted to a higher temperature by 40 K, the diffusion constant as calculated from our simulations matches with experimental values

To understand the vibrational dynamics of MP2 water, we calculate the density of states (VDOS) from the Fourier Transform of the velocity-velocity auto-correlation function at different temperatures as shown in Fig. 5. The increase in temperature significantly optimizes the diffusion coefficient, while having the opposite effect on the vibrational density of states (VDOS). At 340 K, the VDOS shows a greater blue shift compared to 300 K, observed in both classical and quantum simulations in the high-frequency range. This is because the strength of hydrogen bonds weakens as the temperature rises. Classical and Quantum simulations give qualitatively similar VDOS around the lower frequency librational band (˜500 cm^{-1}), with a slight redshift compared to the experiment. The differences between the two simulations are primarily reflected in O–H stretching and H–O–H bending modes. Classical simulations predict the bend peak at ˜1693 cm^{-1} at room temperature, overestimating the blue-shift by approximately 40 cm^{-1} compared to experiment, whereas NQEs shift the peak to 1624 cm^{-1}, showing a smaller discrepancy with the experimental results stretching modes are predicted to experience a blue shift in both simulations, with peaks at 3685 and 3524 cm^{-1} in the classical and quantum simulations, respectively, which also shows that the quantum simulation results are also closer to the experimental data [89]. While MP2 calculations demonstrate excellent agreement with experimental data, that of revPBE0-D3 water somewhat exhibits even superior concordance, particularly for the O–H stretching peak [45].

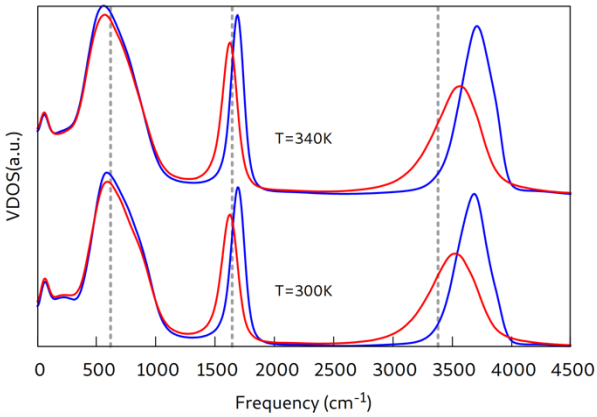

Figure 5. Temperature dependent vibrational density of states at 300 K and 340 K. The blue lines are obtained from classical simulations, while the red lines are from TRPMD. Vertical lines show experimental vibrational frequencies at 300K.

4. Conclusions

In this work, we simulated MP2 water using an NNP at different temperatures using classical and quantum dynamics. MP2 theory, though belonging to the fifth rung of the electronic structure "Jacob's ladder", is unable to predict accurately the static and dynamical properties of liquid water. This may be because an insufficiently large basis set causes MP2 theory to overestimate the Van der Waals interaction. This may be im- proved upon by increasing the basis set to quadruple-ζ and larger, or by estimating the difference between

the results of small and large basis sets using cluster models and decomposing the error into two- and three-body interaction terms, which can be used to further cancel the basis-set error. Alternatively, double-hybrid density functionals based on MP2 and random-phase approximation may be used to train the NNP: they exhibit faster convergence with basis set size at similar computational cost as the parent correlated methods [90].

Although NQEs reduce the height of the first peak of the oxygen-oxygen radial distribution function at room temperature, the match with the experimental RDF is still not perfect [68]. However, a better agreement with experimental RDFs is observed at an elevated temperature of 340 K, at which MP2 predicts stratifying static properties of liquid water compared to the experimental data, as characterized by the RDFs, triplet angles distribution, and tetrahedral local order parameters. It is possible that the elevated temperature cancels the error due to an insufficient basis set, higher kinetic energy compensating for the overestimation of dispersion by MP2 theory.

Our NNP accurately captures a range of static and dynamical properties, while many properties of water such as the dielectric constant and vibrational spectra are still not perfect. Future work will focus on the modelling of these properties using symmetry- adapted machine learning methods [91]. Other future prospects include clarifying the basis set effect on the computed properties, probing the performance of double-hybrid density functionals, and extending simulations to other important simple liquids such as ammonia and hydrogen sulfide.

Acknowledgements

This work was supported by the Swiss National Science Foundation (SNSF) Sinergia grant and the University Research Priority Program (URPP) “LightChEC” of the University of Zurich, focused on solar light to chemical energy conversion. Additional support was provided by the Swiss National Supercomputing Centre (CSCS) under Project IDs uzh1 and s1043. VRR acknowledges funding from the SNSF through an Ambizione grant (No. PZ00P2 174227). J.L. acknowledges support from the National Natural Science Foundation of China (Grant No. 22402128).

References

[1] Pettersson L.G.M., Henchman R.H., Nilsson A., Water: the most anomalous liquid. *Chem. Rev.*, **116** (2016), 7459-7462

[2] Gallo P., Amann-Winkel K., Angell C.A., Anisimov M.A., Caupin F., Chakravarty C., Lascaris E., Loerting T., Panagiotopoulos A.Z., Russo J., et al., Water: a tale of two liquids. *Chem. Rev.*, **116** (2016), 7463-7500

[3] Cisneros G.A., Wikfeldt K.T., Ojamae L., Lu J., Xu Y., Torabifard H., Bartok A.P., Csanyi G., Molinero V., Paesani F., Modeling molecular interactions in water: from pairwise to many-body potential energy functions. *Chem. Rev.*, **116** (2016), 7501-7528

[4] Bakker H.J., Skinner J.L., Vibrational spectroscopy as a probe of structure and dynamics in liquid water. *Chem. Rev.*, **110** (2010), 1498-1517

[5] Smith J.D., Cappa C.D., Wilson K.R., Cohen R.C., Geissler P.L., Saykally R.J., Unified description of temperature-dependent hydrogen-bond rearrangements in liquid water. *Proc. Nat. Acad. Sci.*, **102** (2005), 14171-14174

[6] Wernet P., Nordlund D., Bergmann U., Cavalleri M., Odelius M., Ogasawara H., Näslund L., Hirsch T.K., Ojamae L., Glatzel P., Pettersson L.G.M., Nilsson A., The structure of the first coordination shell in liquid water. *Science*, **304** (2004), 995-999

[7] Nilsson A., Pettersson L.G.M., The structural origin of anomalous properties of liquid water. *Nat. Commun.*, **6** (2015), 8998

[8] Ropp J., Lawrence C., Farrar T.C., Skinner J.L., Rotational motion in liquid water is anisotropic: a nuclear magnetic resonance and molecular dynamics simulation study. *J. Am. Chem. Soc.*, **123** (2001), 8047-8052

[9] Rahman A., Stillinger F.H., Molecular dynamics study of liquid water. *J. Chem. Phys.*, **55** (1971), 3336-3359

[10] Morrone J.A., Car R., Nuclear quantum effects in water. *Phys. Rev. Lett.*, **101** (2008), 017801

[11] Laasonen K., Sprik M., Parrinello M., Car R., Ab initio liquid water. *J. Chem. Phys.*, **99** (1993), 9080-9089

[12] Yu Q., Qu C., Houston P.L., Conte R., Nandi A., Bowman J.M., q-AQUA: a many-body CCSD(T) water potential, including four-body interactions, demonstrates the quantum nature of water from clusters to the liquid phase. *J. Phys. Chem. Lett.*, **13** (2022), 5068-5074

[13] Yu Q., Qu C., Houston P.L., Nandi A., Pandey P., Conte R., Bowman J.M., A status report on “gold standard” machine-learned potentials for water. *J. Phys. Chem. Lett.*, **14** (2023), 8077-8087

[14] Qu C., Yu Q., Houston P.L., Conte R., Nandi A., Bowman J.M., Interfacing q-aqua with a polarizable force field: the best of both worlds. *J. Chem. Theory Comput.*, **19** (2023), 3446-3459

[15] Lu Q., He X., Hu W., Chen X., Liu J., Stability, vibrations, and diffusion of hydrogen gas in clathrate hydrates: insights from ab initio calculations on condensed-phase crystalline structures. *J. Phys. Chem. C*, **123** (2019), 12052-12061

[16] Liu J., Liu Y., Yang J., Zeng X.C., He X., Directional proton transfer in the reaction of the simplest Criegee intermediate with water involving the formation of transient H_3O^+. *J. Phys. Chem. Lett.*, **12** (2021), 3379-3386

[17] Liu J., Lan J., He X., Toward high-level machine learning potential for water based on quantum fragmentation and neural networks. *J. Phys. Chem. A*, **126** (2022), 3926-3936

[18] Liu J., Yang J., Zeng X.C., Xantheas S.S., Yagi K., He X., Towards complete assignment of the infrared spectrum of the protonated water cluster $H^+(H_2O)_{21}$. *Nat. Commun.*, **12** (2021), 6141

[19] Liu J., Zhang J.Z., He X., Probing the ion-specific effects at the water/air interface and water-mediated ion pairing in sodium halide solution with ab initio molecular dynamics. *J. Phys. Chem. B*, **122** (2018), 10202-10209

[20] Liu J., He X., Zhang J.Z., Structure of liquid water – a dynamical mixture of tetrahedral and ring-and-chain-like structures. *Phys. Chem. Chem. Phys.*, **19** (2017), 11931-11936

[21] Hockney R.W., Eastwood J.W., Computer Simulation Using Particles, Hilger: Bristol, 1988.

[22] Mahoney M.W., Jorgensen W.L., Diffusion constant of the TIP5P model of liquid water. *J. Chem. Phys.*, **114** (2001), 363-366

[23] Horn H.W., Swope W.C., Pitera J.W., Madura J.D., Dick T.J., Hura G.L., Head-Gordon T., Development of an improved four-site water model for biomolecular simulations: TIP4P-Ew. *J. Chem. Phys.*, **120** (2004), 9665-9678

[24] Berendsen H., Grigera J., Straatsma T., The missing term in effective pair potentials. *J. Phys. Chem.*, **91** (1987), 6269-6271

[25] Berendsen H.J., Postma J.P., van Gunsteren W.F., Hermans J., Interaction models for water in relation to protein hydration, in *Intermolecular Forces*, Springer, 1981, 331-342.

[26] Babin V., Medders G.R., Paesani F., Development of a first-principles water potential with flexible monomers. II: trimer potential energy surface, third virial coefficient, and small clusters. *J. Chem. Theory Comput.*, **10** (2014), 1599-1607

[27] Gillan M.J., Alfe D., Michaelides A., Perspective: how good is DFT for water? *J. Chem. Phys.*, **144** (2016), 130901

[28] Liberatore E., Meli R., Rothlisberger U., A versatile multiple time step scheme for efficient ab initio molecular dynamics simulations. *J. Chem. Theory Comput.*, **14** (2018), 2834-2842

[29] Yoo S., Zeng X.C., Xantheas S.S., On the phase diagram of water with density functional theory potentials: the melting temperature of ice Ih with the Perdew–Burke–Ernzerhof and Becke–Lee–Yang–Parr functionals. *J. Chem. Phys.*, **130** (2009), 221102

[30] Forster-Tonigold K., Groß A., Dispersion corrected RPBE studies of liquid water. *J. Chem. Phys.*, **141** (2014), 064501

[31] Bankura A., Karmakar A., Carnevale V., Chandra A., Klein M.L., Structure, dynamics, and spectral diffusion of water from first-principles molecular dynamics. *J. Phys. Chem. C*, **118** (2014), 29401-29411

[32] Yoo S., Xantheas S.S., Communication: the effect of dispersion corrections on the melting temperature of liquid water. *J. Chem. Phys.*, **134** (2011), 121105

[33] Rybkin V.V., Sampling potential energy surfaces in the condensed phase with many-body electronic structure methods. *Chem.–Eur. J.*, **26** (2019), 362-368

[34] Sun J., Ruzsinszky A., Perdew J.P., Strongly constrained and appropriately normed semilocal density functional. *Phys. Rev. Lett.*, **115** (2015), 036402

[35] Chen M., Ko H.-Y., Remsing R.C., Andrade M.F.C., Santra B., Sun Z., Selloni A., Car R., Klein M.L., Perdew J.P., et al., Ab initio theory and modeling of water. *Proc. Nat. Acad. Sci.*, **114** (2017), 10846-10851

[36] Dasgupta S., Lambros E., Perdew J.P., Paesani F., Elevating density functional theory to chemical accuracy for water simulations through a density-corrected many-body formalism. *Nat. Commun.*, **12** (2021), 1-12

[37] Wiktor J., Ambrosio F., Pasquarello A., Note: assessment of the SCAN+ rVV10 functional for the structure of liquid water. *J. Chem. Phys.*, **147** (2017), 216101

[38] Pestana L.R., Mardirossian N., Head-Gordon M., Head-Gordon T., Ab initio molecular dynamics simulations of liquid water using high quality meta-GGA functionals. *Chem. Sci.*, **8** (2017), 3554-3565

[39] Marsalek O., Markland T.E., Quantum dynamics and spectroscopy of ab initio liquid water: the interplay of nuclear and electronic quantum effects. *J. Phys. Chem. Lett.*, **8** (2017), 1545-1551

[40] Cheng B., Engel E.A., Behler J., Dellago C., Ceriotti M., Ab initio thermodynamics of liquid and solid water. *Proc. Nat. Acad. Sci.*, **116** (2019), 1110-1115

[41] Ambrosio F., Miceli G., Pasquarello A., Structural, dynamical, and electronic properties of liquid water: a hybrid functional study. *J. Phys. Chem. B*, **120** (2016), 7456-7470

[42] Del Ben M., Schönherr M., Hutter J., VandeVondele J., Bulk liquid water at ambient temperature and pressure from MP2 theory. *J. Phys. Chem. Lett.*, **4** (2013), 3753-3759

[43] Willow S.Y., Zeng X.C., Xantheas S.S., Kim K.S., Hirata S., Why is MP2-water "cooler" and "denser" than DFT-water? *J. Phys. Chem. Lett.*, **7** (2016), 680-684

[44] Ceriotti M., Fang W., Kusalik P.G., McKenzie R.H., Michaelides A., Morales M.A., Markland T.E., Nuclear quantum effects in water and aqueous systems: experiment, theory, and current challenges. *Chem. Rev.*, **116** (2016), 7529-7550

[45] Markland T.E., Ceriotti M., Nuclear quantum effects enter the mainstream. *Nat. Rev. Chem.*, **2** (2018), 1-14

[46] Li X., Walker B., Michaelides A., Quantum nature of the hydrogen bond. *Proc. Nat. Acad. Sci. U.S.A.*, **108** (2011), 6369-6373

[47] Habershon S., Markland T.E., Manolopoulos D.E., Competing quantum effects in the dynamics of a flexible water model. *J. Chem. Phys.*, **131** (2009), 024501

[48] Li C., Paesani F., Voth G.A., Static and dynamic correlations in water: comparison of classical ab initio molecular dynamics at elevated temperature with path integral simulations at ambient temperature. *J. Chem. Theory Comput.*, **18** (2022), 2124-2131

[49] Lan J., Rybkin V.V., Iannuzzi M., Ionization of water as an effect of quantum delocalization at aqueous electrode interfaces. *J. Phys. Chem. Lett.*, **11** (2020), 3724-3730

[50] Rybkin V.V., VandeVondele J., Nuclear quantum effects on aqueous electron attachment and redox properties. *J. Phys. Chem. Lett.*, **8** (2017), 1424-1428

[51] Parrinello M., Rahman A., Study of an F center in molten KCl. *J. Chem. Phys.*, **80** (1984), 860-867

[52] Behler J., Parrinello M., Generalized neural-network representation of high-dimensional potential-energy surfaces. *Phys. Rev. Lett.*, **98** (2007), 146401

[53] Zhang L., Han J., Wang H., Car R., Weinan E., Deep potential molecular dynamics: a scalable model with the accuracy of quantum mechanics. *Phys. Rev. Lett.*, **120** (2018), 143001

[54] Shepherd S., Lan J., Wilkins D.M., Kapil V., Efficient quantum vibrational spectroscopy of water with high-order path integrals: from bulk to interfaces. *J. Phys. Chem. Lett.*, **12** (2021), 9108-9114

[55] Kapil V., Wilkins D.M., Lan J., Ceriotti M., Inexpensive modeling of quantum dynamics using path integral generalized Langevin equation thermostats. *J. Chem. Phys.*, **152** (2020), 124104

[56] Yao Y., Kanai Y., Nuclear quantum effect and its temperature dependence in liquid water from random phase approximation via artificial neural network. *J. Phys. Chem. Lett.*, **12** (2021), 6354-6362

[57] Lan J., Kapil V., Gasparotto P., Ceriotti M., Iannuzzi M., Rybkin V.V., Simulating the ghost: quantum dynamics of the solvated electron. *Nat. Commun.*, **12** (2021), 1-6

[58] Kapil V., Rossi M., Marsalek O., Petraglia R., Litman Y., Spura T., Cheng B., Cuzzocrea A., Meißner R.H., Wilkins D.M., et al., i-pi 2.0: a universal force engine for advanced molecular simulations. *Comput. Phys. Commun.*, **236** (2019), 214-223

[59] Ceriotti M., More J., Manolopoulos D.E., i-pi: a Python interface for ab initio path integral molecular dynamics simulations. *Comput. Phys. Commun.*, **185** (2014), 1019-1026

[60] Plimpton S., Fast parallel algorithms for short-range molecular

dynamics. *J. Comput. Phys.*, **117** (1995), 1-19

[61] Singraber A., Behler J., Dellago C., Library-based LAMMPS implementation of high-dimensional neural network potentials. *J. Chem. Theory Comput.*, **15** (2019), 1827-1841

[62] Bussi G., Donadio D., Parrinello M., Canonical sampling through velocity rescaling. *J. Chem. Phys.*, **126** (2007), 014101

[63] Rossi M., Ceriotti M., Manolopoulos D.E., How to remove the spurious resonances from ring polymer molecular dynamics. *J. Chem. Phys.*, **140** (2014), 234116

[64] Kapil V., Cuzzocrea A., Ceriotti M., Anisotropy of the proton momentum distribution in water. *J. Phys. Chem. B*, **122** (2018), 6048-6054

[65] Ceriotti M., Parrinello M., Markland T.E., Manolopoulos D.E., Efficient stochastic thermostatting of path integral molecular dynamics. *J. Chem. Phys.*, **133** (2010), 124104

[66] Benson R.L., Trenins G., Althorpe S.C., Which quantum statistics–classical dynamics method is best for water? *Faraday Discuss.*, **221** (2019), 350-366

[67] Dehaoui A., Issenmann B., Caupin F., Viscosity of deeply supercooled water and its coupling to molecular diffusion. *Proc. Nat. Acad. Sci.*, **112** (2015), 12020-12025

[68] Del Ben M., Hutter J., VandeVondele J., Probing the structural and dynamical properties of liquid water with models including non-local electron correlation. *J. Chem. Phys.*, **143** (2015), 054506

[69] Sugita Y., Okamoto Y., Replica-exchange molecular dynamics method for protein folding. *Chem. Phys. Lett.*, **314** (1999), 141-151

[70] Imbalzano G., Anelli A., Giofré D., Klees S., Behler J., Ceriotti M., Automatic selection of atomic fingerprints and reference configurations for machine-learning potentials. *J. Chem. Phys.*, **148** (2018), 241730

[71] Del Ben M., Hutter J., VandeVondele J., Forces and stress in second-order Møller-Plesset perturbation theory for condensed phase systems within the resolution-of-identity Gaussian and plane waves approach. *J. Chem. Phys.*, **143** (2015), 102803

[72] Rybkin V.V., VandeVondele J., Spin-unrestricted second-order Møller–Plesset (MP2) forces for the condensed phase: from molecular radicals to F-centers in solids. *J. Chem. Theory Comput.*, **12** (2016), 2214-2223

[73] Del Ben M., Hutter J., VandeVondele J., Electron correlation in the condensed phase from a resolution of identity approach based on the Gaussian and plane waves scheme. *J. Chem. Theory Comput.*, **9** (2013), 2654-2671

[74] Hutter J., Iannuzzi M., Schiffmann F., VandeVondele J., CP2K: atomistic simulations of condensed matter systems. *Wiley Interdiscip. Rev. Comput. Mol. Sci.*, **4** (2014), 15-25

[75] Kühne T.D., Iannuzzi M., Del Ben M., Rybkin V.V., Seewald P., Stein F., Laino T., Khaliullin R.Z., Schütt O., Schiffmann F., Golze D., Wilhelm J., Chulkov S., Bani-Hashemian M.H., Weber V., Borštnik U., Taillefumier M., Jakobovits A.S., Lazzaro A., Pabst H., Müller T., Schade R., Guidon M., Andermatt S., Holmberg N., Schenter G.K., Hehn A., Bussy A., Belleflamme F., Tabacchi G., Glöß A., Lass M., Bethune I., Mundy C.J., Plessl C., Watkins M., VandeVondele J., Krack M., Hutter J., CP2K: an electronic structure and molecular dynamics software package – Quickstep: efficient and accurate electronic structure calculations. *J. Chem. Phys.*, **152** (2020), 194103

[76] Reddy S.K., Straight S.C., Bajaj P., Pham C.H., Riera M., Moberg D.R., Morales M.A., Knight C., Götz A.W., Paesani F., On the accuracy of the MB-pol many-body potential for water: interaction energies, vibrational frequencies, and classical thermodynamic and dynamical properties from clusters to liquid water and ice. *J. Chem. Phys.*, **145** (2016), 194504

[77] Wagner W., Pruß A., The IAPWS formulation 1995 for the thermodynamic properties of ordinary water substance for general and scientific use. *J. Phys. Chem. Ref. Data*, **31** (2002), 387-535

[78] Skinner L.B., Huang C., Schlesinger D., Pettersson L.G., Nilsson A., Benmore C.J., Benchmark oxygen-oxygen pair-distribution function of ambient water from X-ray diffraction measurements with a wide Q-range. *J. Chem. Phys.*, **138** (2013), 074506

[79] Soper A., Benmore C., Quantum differences between heavy and light water. *Phys. Rev. Lett.*, **101** (2008), 065502

[80] Kim J., Kim K.S., Structures, binding energies, and spectra of isoenergetic water hexamer clusters: extensive ab initio studies. *J. Chem. Phys.*, **109** (1998), 5886-5895

[81] Xantheas S.S., Burnham C.J., Harrison R.J., Development of transferable interaction models for water. II: accurate energetics of the first few water clusters from first principles. *J. Chem. Phys.*, **116** (2002), 1493-1499

[82] Xantheas S.S., Aprà E., The binding energies of the D2d and S4 water octamer isomers: high-level electronic structure and empirical potential results. *J. Chem. Phys.*, **120** (2004), 823-828

[83] Temelso B., Archer K.A., Shields G.C., Benchmark structures and binding energies of small water clusters with anharmonicity corrections. *J. Phys. Chem. A*, **115** (2011), 12034-12046

[84] Miliordos E., Aprà E., Xantheas S.S., Optimal geometries and harmonic vibrational frequencies of the global minima of water clusters $(H_2O)_n$, n = 2–6, and several hexamer local minima at the CCSD(T) level of theory. *J. Chem. Phys.*, **139** (2013), 114302

[85] Liu J., He X., Zhang J.Z., Qi L.-W., Hydrogen-bond structure dynamics in bulk water: insights from ab initio simulations with coupled cluster theory. *Chem. Sci.*, **9** (2018), 2065-2073

[86] Liu J., He X., Zhang J.Z., Zhang J.Z.H., Structure of liquid water – a dynamical mixture of tetrahedral and ring-and-chain-like structures. *Phys. Chem. Chem. Phys.*, **19** (2017), 11931-11936

[87] Yeh I.-C., Hummer G., System-size dependence of diffusion coefficients and viscosities from molecular dynamics simulations with periodic boundary conditions. *J. Phys. Chem. B*, **108** (2004), 15873-15879

[88] Tofts P., Lloyd D., Clark C., Barker G., Parker G., McConville P., Baldock C., Pope J., Test liquids for quantitative MRI measurements of self-diffusion coefficient in vivo. *Magn. Reson. Med.*, **43** (2000), 368-374

[89] Chase M.W., NIST-JANAF Thermochemical Tables, *J. Phys. Chem. Ref. Data* Monograph 9, 1998.

[90] Stein F., Hutter J., Rybkin V.V., Double-hybrid DFT functionals for the condensed phase: Gaussian and plane waves implementation and evaluation. *Molecules*, **25** (2020), 5174

[91] Grisafi A., Wilkins D.M., Csányi G., Ceriotti M., Symmetry-adapted machine learning for tensorial properties of atomistic systems. *Phys. Rev. Lett.*, **120** (2018), 036002